

# Ultrasound excited thermography using frequency modulated elastic waves

Th. Zweschper<sup>1</sup>, A. Dillenz<sup>2</sup>, G. Riegert<sup>1</sup>, D. Scherling<sup>3</sup> and G. Busse<sup>1</sup>

<sup>1</sup>University of Stuttgart – Institute of Polymer Testing and Polymer Science (IKP),  
Department of Non-destructive Testing,  
Pfaffenwaldring 32, D-70569 Stuttgart, Germany  
(zweschper@ikp.uni-stuttgart.de)

<sup>2</sup>e/de/vis – enhanced defect visualization, Einsteinstr. 14, D-71229 Leonberg, Germany

<sup>3</sup>Airbus Germany GmbH, Huenefeldstrasse 1-5, D-28199 Bremen, Germany

Ultrasound excited thermography allows for defect selective imaging using thermal waves that are generated by elastic waves. The mechanism involved is local friction or hysteresis which turns a dynamically loaded defect into a heat source which is identified by a thermography system. If the excitation frequency matches to a resonance of the vibrating system, temperature patterns can occur that are caused by standing elastic waves. This undesirable patterns can affect the detection of damages in a negative way. We describe a technique how the defect detectability of ultrasound activated thermography can be improved. With the objective of a preferably diffuse distributed sonic field we applied frequency modulated ultrasound to the material. That way the standing waves can be eliminated or reduced and the detectability is improved.

## 1 Introduction

Reliable inspection techniques are required for the maintenance of safety relevant structures (e.g. aerospace equipment and vehicles) where one needs to detect defect areas early enough to prevent catastrophic failure. As many structures consist of carbon fibre reinforced plastics (CFRP), the rapid and remote identification of delamination, impact damages, ruptures, and cracks is a topic of major concern. Therefore a method is required that is applicable during inspection procedures to monitor the integrity of such structures.

## 2 External excitation: Optical Lockin Thermography (OLT)

Thermal waves (1) have been used very early for remote monitoring of thermal features, e.g. cracks, delamination (2), and other kinds of boundaries. After the advantage of signal phase had been discovered (3-5), phase angle imaging using photothermal techniques (6) became a powerful tool for imaging of hidden structures due to the enhanced depth range and its independence on optical (7) or infrared surface patterns. As the thermal diffusion length is the important parameter for depth range (8), it turned out very soon that imaging of features deep underneath the surface requires very low modulation frequencies and a correspondingly long time to obtain a photothermal image. Unfortunately many industrial questions are related to samples with defects at about a millimetre depth. An image obtained pixel after pixel at a modulation frequency in the 1 Hz range could easily require several hours.

One approach allowing for a reduction of inspection time is lockin thermography where the low frequency thermal wave is generated simultaneously on the whole surface of the inspected component and monitored everywhere several times per modulation cycle in order to obtain an image of amplitude and phase of temperature modulation (9-12). In this case the inspection time is given by a few modulation cycles. As one can image square meters of airplanes within a few minutes (13), one has a powerful method for fast inspection of safety relevant structures with a depth range of several millimetres in CFRP.

Figure 1 shows the principle and the set-up of optical excited lockin thermography. Absorption of intensity modulated radiation generates on the whole surface a thermal wave. It propagates into the interior where it is reflected at boundaries and defects so that it moves back to the surface where it is superposed to the initial wave. This way a defect is revealed by the local change of phase angle.

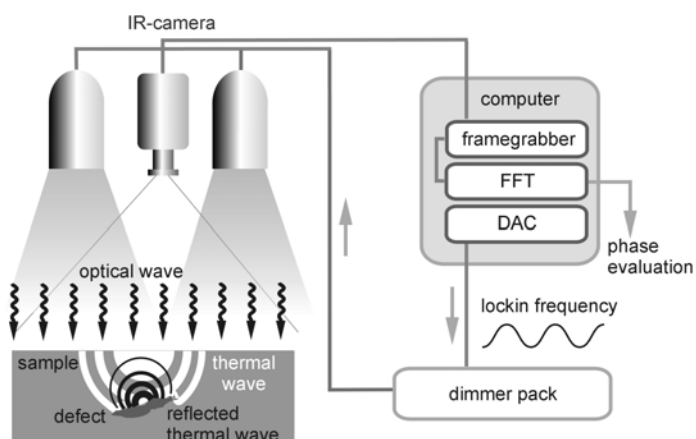


Figure 1. Principle and set-up of lockin thermography with optical excitation.

Therefore both defects and intact structures are imaged at the same time. Defects can be revealed only by comparing the observed features with expected patterns provided by theory, by reference samples, or by design drawings. Even for an experienced inspector it is difficult to distinguish defect areas from these thermal features.

### 3 Internal excitation methods

Further investigations aimed at a method where a defect responds selectively so that the image would display only the defect and not the confusing background of the intact structure. Defects differ from their surroundings by their mechanical weakness. They may cause stress concentrations, and under periodical load there may be hysteresis effects or friction in cracks and delamination. As defects may be areas where mechanical damping is enhanced, the ultrasound is converted into heat mainly in defects (14, 15).

#### 3.1 Ultrasound Lockin Thermography (ULT)

Modulation of the elastic wave amplitude results in periodical heat generation so that the defect is turned into a local thermal wave transmitter. Its emission is detected via the temperature modulation at the surface which is analysed by lockin thermography tuned to the frequency of amplitude modulation (16). The ultrasonic transducer is attached at a fixed spot from where the acoustic waves are launched into the whole volume where they are reflected several times until they disappear preferably in a defect and generate heat. These high frequencies are very efficient in heating since many hysteresis cycles are performed per second.

#### 3.2 Ultrasound Burst Phase Thermography (UBP)

Another established method is the use of short sonic bursts for sample excitation (17). The spectral components of that signal and the following cooling down period provide information about defects in almost the same way as Lockin technique but with reduced measuring duration. As the characteristic defect signal is contained in a limited spectral range while the noise typically is distributed over the whole spectrum, one can reduce noise as well. That kind of evaluation technique using Fourier or Wavelet transformations is also applicable to flash light excited thermography (18-20). The signal to noise ratio of ULT and UBP images (and hence defect detectability) is significantly better than just one temperature snapshot image in a sequence (21, 22).

The following example confirms that high frequencies probe only near-surface areas while low frequencies with their larger depth range provide information about defects deeper inside the component. Thus depth resolved mapping of defects can be performed with only one measurement. For this demonstration we manufactured a sample which had four delaminations in various depths between 0.2 mm and 2.2 mm. After an ultrasonic burst of 200 ms duration (1.1 kW) had been applied the resulting temperature sequence was evaluated at different frequencies. In the phase image at 4 Hz (Figure 2a) only the defect next to the surface causes a change in the phase angle. At 1 Hz (Figure 2b) already three delaminations in depths from 0.2 mm to 1.5 mm become visible. At 0.1 Hz (Figure 2c) all defects appear. At an even lower frequency (0.025 Hz, see Figure 2d) the image contrast is reduced due to lateral diffusion effects.

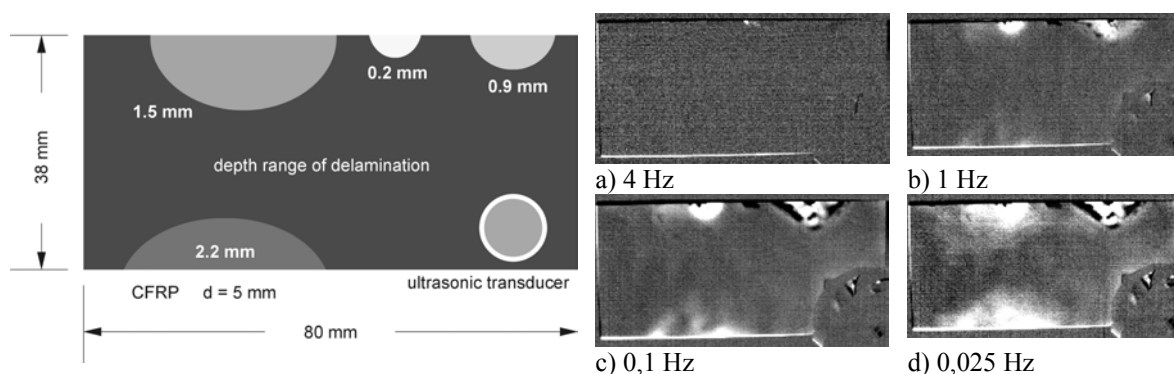


Figure 2. UBP images of a CFRP sample with delamination in different depths. Excitation: 1.1 kW, ultrasonic frequency 20 kHz, burst duration: 200 ms.

### 4 Experimental arrangement

The experimental set-up is shown in figure 3. We used a non-standard 2.2 kW power supply, driving an ultrasonic welding transducer whose excitation frequency can be modulated with a frequency up to 25 Hz in a range from 15 to 25 kHz. The excitation duration typically ranges from 100 ms up to a few seconds for burst phase thermography and up to some minutes for lockin thermography. A digital to analogue converter triggers the modulation frequency and if required the lockin frequency for amplitude modulation. The temperature sequences were acquired with a focal plane array IR camera (CEDIP Jade MWIR). The software (e/de/vis

DisplayIMG) installed on a common personal computer performs an online Fourier transformation and subsequent image processing.

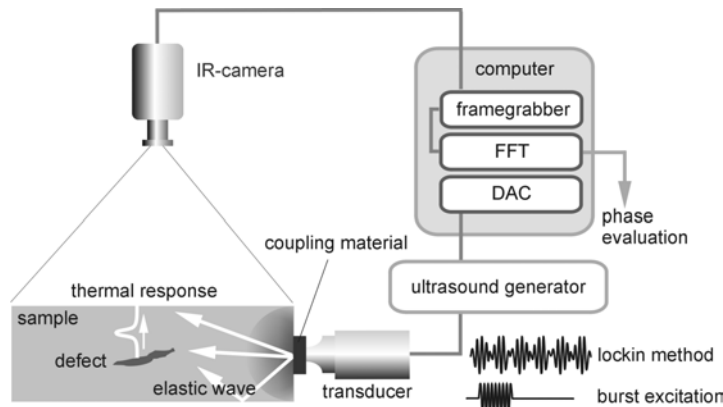


Figure 3. Principle and set-up of ultrasonic excited thermography.

The tip of the welding horn is pressed against the component to be tested (see figure 4). For an efficient ultrasound coupling tight contact as well as impedance matching is important. The acoustic impedance  $Z$  is given by the product of the density  $\rho$  and the elastic wave velocity  $v$  in the material. In close analogy to optical techniques it is advantageous if the acoustic impedance of the coupling material ( $Z_c$ ) matches with the geometric mean of the acoustic impedance of the material to be tested ( $Z_s$ ) and the material of the welding horn ( $Z_h$ ), in our case a titanium base alloy

$$Z_c = \sqrt{Z_s Z_h} = \sqrt{\rho_s v_s \cdot \rho_h v_h} . \quad (1)$$

In terms of optimised ultrasound coupling in CFRP, good results were obtained on a thin sheet of adhesive aluminium tape whose acoustic impedance is close to the square root mentioned above. In comparison to the direct coupling without any coupling material an increase of the efficiency of 35 per cent was achieved. Such materials do not only improve the ultrasound coupling but also the component surface was protected against external damage caused by mechanical and thermal load during the ultrasonic excitation.

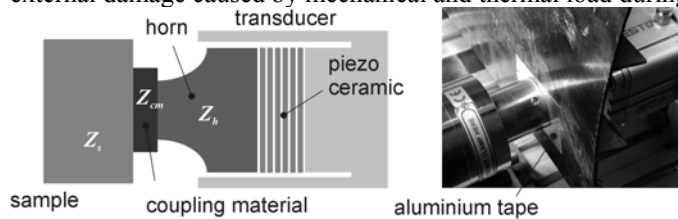


Figure 4. Impedance matching for efficient ultrasound coupling.

## 5 Enhanced defect detectability using frequency modulated ultrasound

By applying a monofrequent excitation to a sample it is not unlikely that this frequency matches to a resonance of the vibrating system. The result is a standing wave pattern. Due to hysteretic losses in the elongation maximum, these standing elastic waves can appear as temperature patterns causing misinterpretations: In the worst case the defect could be hidden in a node ("blind spot") while the standing wave maximum might appear as a defect. This can be avoided by using two or more ultrasound converters with several frequencies simultaneously or, even better, by frequency modulation of a sinusoidal signal. In these cases the standing wave pattern is superimposed by a field of propagating waves giving sensitivity also where only nodes existed before.

An example for the advances of frequency modulated sonic excitation is the inspection of a CFRP plate with nine areas of heat damage at the rear side of the sample (figure 5). The initial sample with a thickness of 2 mm was damaged by thermal overload and subsequently enlarged to a thickness of 5 mm. To localize the nine damages and to characterize their real size respectively an air coupled ultrasound c-scan was performed at 450 kHz (figure 5a). The limited depth range of optically excited lockin thermography prevents a successful application of this remote technique on the laminate: All damages remain undetected (figure 5b). The use of sonic excitation improves the situation. Using the lockin technique with its enlarged depth range five of the nine damages could be found (figure 5c). But the monofrequent excitation ( $f_R = 20$  kHz) generates a temperature pattern caused by standing elastic waves with all the drawbacks mentioned before. Especially the smaller defects remain still undetected. A significant enhancement was achieved by wobbling the excitation frequency from 15 to 25 kHz with a modulation frequency of 20 Hz. The pattern was reduced mostly, now eight of the thermal damage are visible (figure 5d). In this case the modulation of the excitation frequency enhances defect detectability.

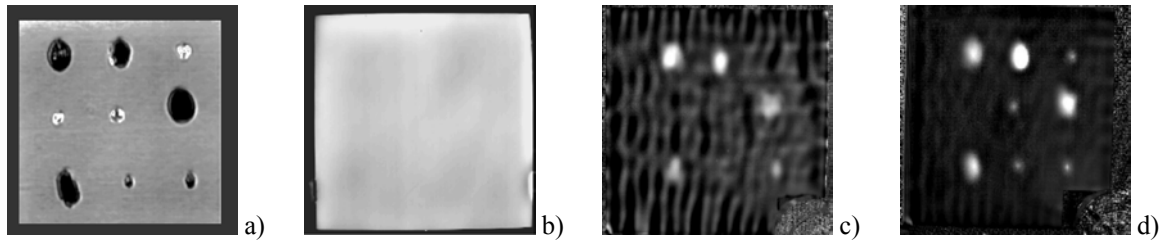
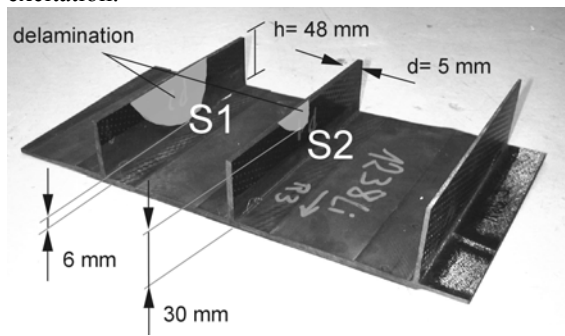


Figure 5. Detection of delamination caused by thermal overload in a CFRP plate ( $d = 5$  mm) using sonic excitation. Comparison of different techniques: a) air coupled ultrasound c-scan (450 kHz), b) phase evaluation of optical excited lockin thermography at a frequency of 0.01 Hz, c) phase signature of ultrasound excited lockin thermography at 0.05 Hz, d) reduced standing wave pattern and increased defect detectability using frequency modulated ultrasound lockin thermography ( $f_R=15 \dots 25$  kHz,  $f_{mod}=20$  Hz), phase signature at 0.05 Hz with.

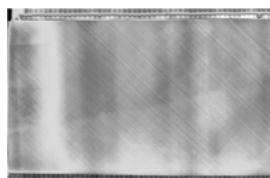
## 6 Detection of fractures, delamination, and cracks in CFRP stringer structures

Fractures of stringers in aerospace components are a serious problem because this kind of damage is almost invisible from the outer surface of an aircraft for most non-destructive testing methods, since stringers are hidden behind a panel. The access from inside the aircraft is difficult and time consuming.

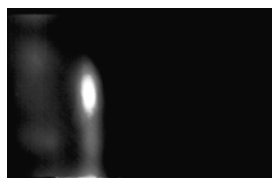
The CFRP structure to be inspected had fractures in its stringers as shown in figure 6a schematically. The damage was covered by a CFRP skin with a thickness of more than 6 mm. While stringer delaminations can be detected with optically excited Lockin Thermography (13), the depth range of optically generated thermal waves is not sufficient to reveal hidden stringer fractures (Figure 6b). Ultrasound Lockin Thermography (Figure 6c and 6d) and Ultrasound Burst Phase image (Figure 6e) can reveal the fracture in the left stringer clearly. The damage in the right stringer is too far from the surface (30 mm), therefore it remains undetected even with sonic excitation.



a) CFRP stringer structure  
thickness of skin: 6 mm.  
Laminated stringer (thickness 5 mm, height 48 mm).  
Fractures are marked white.



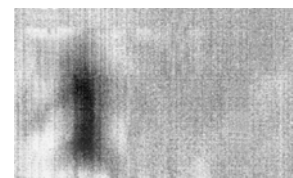
b) Optical Lockin Thermography Phase image at 0.01 Hz, 200 seconds acquisition time



c) Ultrasound Lockin Amplitude image at 0.01 Hz, 400 W, and 100 seconds acquisition time



d) Ultrasound Lockin Phase image at 0.01 Hz, 400 W, and 100 seconds acquisition time



e) Ultrasound Burst Phase image at 0,0485 Hz, burst length 5s, 400 W

Figure 6. Comparison of different phase images of ruptures in a aerospace component

A stringer reinforced structure where we compared several excitation techniques is the cutout of a flap (850 mm x 240 mm) with a crack and a delamination in the stringer underneath the intact CFRP-skin (thickness 4.5 mm). The OLT phase image (figure 7b) suppresses the optical sample characteristics and displays the whole thermal structure of the component (stringer, rib, and variation of material thickness), but the small effect of the defect easily escapes attention. The temperature pattern in the ULT phase signature (figure 7c) caused by standing waves constricts the detection of the crack considerably. When frequency modulated ultrasound ( $f_R = 15 \dots 25$  kHz,  $f_{mod} = 20$  Hz) was applied the pattern disappeared and defect detectability increased significantly (figure 7d).

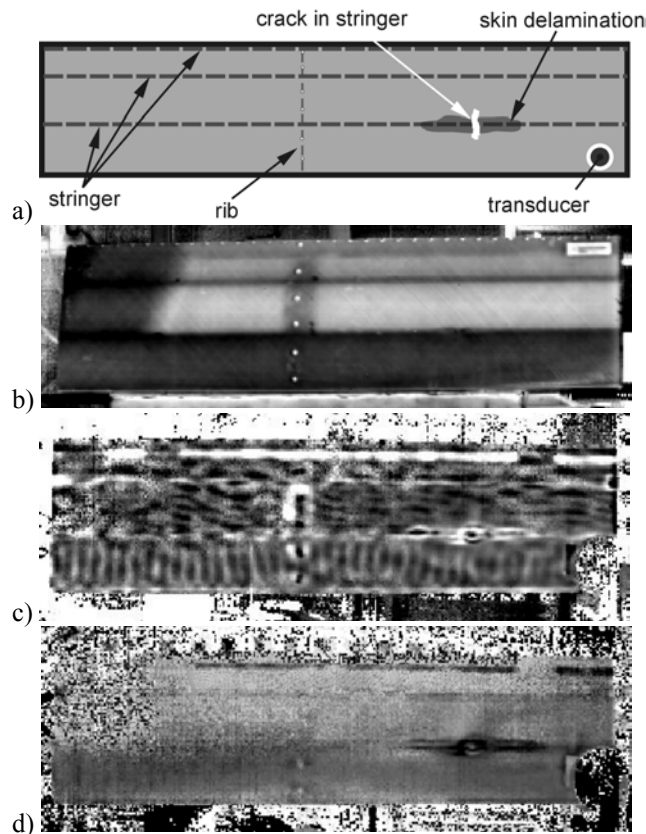


Figure 7. Detection of a crack in a stringer of a CFRP landing flap (cutout) using different techniques: a) map of damage location, b) phase evaluation of optically excited lockin thermography at a frequency of 0.05 Hz, c) phase signature of ultrasound excited lockin thermography at 0.05 Hz. d) elimination of the standing wave pattern using frequency modulated ultrasound lockin thermography, phase signature at 0.05 Hz.

## 7 Damage detection using small piezo-ceramic actuators

From previous investigations it is known that soft materials could be damaged by injecting elastic waves with high energy (24). An alternative approach is the use of many small distributed piezo-ceramic actuators to generate an elastic wave field in the inspected component. This results in a reduction of mechanical and thermal load. Here we examined a thin carbon fibre plate with seven impact damages. Three piezo-ceramic actuators were bonded to the sample to generate a wave field at a frequency of 8 kHz with 200 W for 1 second. Some milliseconds after the excitation burst, the best thermal contrast for defect detection is achieved (figure 8a). However, there is only a small change in temperature at the damaged regions of the sample. The amplitude image calculated with a Fourier transform at 0.24 Hz is an improvement in terms of signal to noise ratio (figure 8b). The defects are displayed with better contrast, but friction between sample and actuators causes thermal fringes around the actuators. This effect is reduced in the phase image (figure 8c), where inhomogeneities of temperature variations are eliminated.

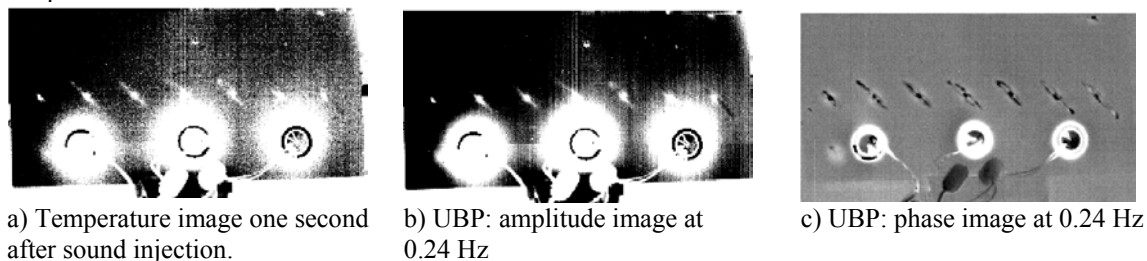


Figure 8. UBP: amplitude and phase image of seven impacts in CFRP ( $d = 2$  mm).

## 8 Conclusion

Ultrasound excited thermography is an efficient non-destructive tool. The phase evaluation of the recorded temperature sequences has clear advantages as compared to conventional pulse thermography: Sensitivity variations within the detector array as well as optical sample characteristics such as inhomogeneous temperature distribution and varying emission coefficients on the sample surface are suppressed. Furthermore the signal to noise ratio is improved significantly. The use of short sonic bursts for sample excitation in conjunction with phase evaluation reduce the measuring time without abandoning the advantages mentioned before. Automation is possible, a cycle time less than one second per measurement is achieved.

Coupling materials for impedance matching do not only improve the ultrasound coupling but also the component surface was protected against external damage caused by mechanical and thermal load during the ultrasonic excitation. By applying a frequency modulated ultrasonic excitation the disturbing temperature patterns caused by standing elastic waves were eliminated. This results in homogenous power density in the material and in an increased defect detectability.

However, the high excitation power contained in short pulses or bursts may cause damage to the inspected structure. The simultaneous use of several ultrasound converters provides a more homogenous low power density in the material to be inspected. This results in an efficient and non-destructive excitation so that even larger components can be examined with this technique.

## 9 Acknowledgements

The authors are grateful to Airbus Deutschland GmbH (Bremen, Germany) for their helpful cooperation and for providing samples. Technical support of CEDIP Infrared Systems (Croissy-Beaubourg, France) is highly appreciated as well.

## 10 References

1. Fourier J.: Théorie du mouvement de la chaleur dans les corps solides, 1re Partie. In: Mémoires de l'Académie des Sciences 4 (1824) pp.185-555.
2. Wong Y. H.; Thomas R. L.; Pouch J. J.: Subsurface structures of solids by scanning photoacoustic microscopy. In: Appl. Phys. Lett. 35 5 (1979) pp. 368-369.
3. Busse G.: Optoacoustic phase angle measurement for probing a metal. In: Appl. Phys. Lett. Vol. 35 (1979) pp. 759-760.
4. Thomas R. L.; Pouch J. J.; Wong Y. H.; Favro L. D.; Kuo P. K.; Rosencwaig A.: Subsurface flaw detection in metals by photoacoustic microscopy. In: J. Appl. Phys. Vol. 51 (1980): pp. 1152-1156.
5. Lehto A.; Jaarinen J.; Tiisanen T.; Jokinen M.; Luukkala M.: Amplitude and phase in thermal wave imaging. In: Electr. Lett. Vol. 17 (1981): pp. 364-365.
6. Nordal, P.-E.; Kanstad S.O.: Photothermal radiometry. In: Physica Scripta Vol. 20 (1979): pp. 659-662.
7. Rosencwaig A.; Busse G.: High resolution photoacoustic thermal wave microscopy. In: Appl. Phys. Lett. Vol. 36 (1980): pp. 725-727.
8. Rosencwaig A.: Photoacoustic microscopy. In: American Lab. 11 (1979) pp. 39-49.
9. Carlomagno G. M.; Berardi P. G.: Unsteady thermotopography in non-destructive testing. In: Proc. 3<sup>rd</sup> Biannual Exchange, St. Louis/USA, 24.-26. August 1976, pp. 33-39.
10. Beaudoin J. L.; Merienne E.; Danjoux R.; Egee M.: Numerical system for infrared scanners and application to the subsurface control of materials by photothermal radiometry. In: Infrared Technology and Applications, SPIE Vol. 590 (1985) p. 287.
11. Kuo, P.K.; Feng Z. J.; Ahmed T.; Favro L. D.; Thomas R. L.; Hartikainen J.: Parallel thermal wave imaging using a vector lock-in video technique. In: Photoacoustic and Photothermal Phenomena, ed. P. Hess and J. Pelzl. Heidelberg: Springer-Verlag. (1987) pp. 415-418.
12. Busse, G., Wu D. and Karpen W.: Thermal wave imaging with phase sensitive modulated thermography. In: J. Appl. Phys. Vol. 71 (1992): pp. 3962-3965.
13. Wu, D.; Salerno A.; Malter U.; Aoki R.; Kochendörfer R.; Kächele P. K.; Woithe K.; Pfister K.; Busse G.: Inspection of aircraft structural components using lockin-thermography. In: Quantitative infrared thermography, QIRT 96, Stuttgart, ed. D. Balageas, G. Busse, and G. M. Carlomagno. Pisa: Edizione ETS (1997): pp. 251-256. ISBN 88 - 467 - 0089 - 9
14. Mignogna R. B.; Green R. E., Jr.; Duke; Henneke E. G.; Reifsnider K.L.: Thermographic investigations of high-power ultrasonic heating in materials. In: Ultrasonics 7 (1981) pp. 159-163.
15. Stärk F.: Temperature measurements on cyclically loaded materials. In: Werkstofftechnik 13, Verlag Chemie GmbH, Weinheim (1982) pp. 333-338.
16. Rantala J.; Wu D.; Busse G.: Amplitude Modulated Lock-In Vibrothermography for NDE of Polymers and Composites. In: Research in Nondestructive Evaluation, Vol. 7 (1996) pp. 215-218.
17. Patent DE 100 59 854.4
18. Maldague, X.; Marinetti, S.; Pulse Phase Infrared Thermography, J. Appl. Phys, 79 [5]: 2694-2698, 1 March 1996.
19. F. Galmiche, S. Vallerand, X. Maldague, Pulsed Phase Thermography with the Wavelet Transform, Review of Progress in Quantitative NDE, D.O. Thompson et D.E. Chimenti eds, Am. Institute of Physics, 19A: S. 609-615, (Montréal Juli 1999), 2000.
20. Maldague, X.; Marinetti, S.; Busse, G.; Couturier, J.-P.: Possible applications of pulse phase thermography. Progress in Natural Science. Supplement to Vol. 6, December 1996, S. 80-82
21. L. D. Favro, Xiaoyan Han, Zhong Ouyang, Gang Sun, Hua Sui, and R. L. Thomas, Infrared imaging of defects heated by a sonic pulse, Rev. Sci. Inst. 71, 6, 2000, S. 2418-2421.

22. R. L. Thomas, L.D. Favro, P. K. Kuo, T. Ahmed, Xiaoyan Han, Li Wang, Xun Wang and S.M. Shepard, Pulse-Echo Thermal-Wave Imaging for Non-Destructive Evaluation, Proc. 15th International Congress on Acoustics, Trondheim, Norway, June 26-30, 1995, S. 433-436.
23. Salerno, A.; Dillenz, A.; Wu, D.; Rantala, J.; Busse; G.: Progress in ultrasonic lockin thermography. Quantitative infrared thermography, QIRT 98. Akademickie Centrum Graficzno-Marketingowe Lodart S.A., Lodz 1998, S. 154-160. ISBN 83-87202-88-6
24. Dillenz, D.; Zweschper, Th.; Busse, G.: Progress in ultrasound phase angle thermography, Thermosense 2001, Orlando, USA.